CHAPTER IV
CONVERSION OF METHYLESTERS TO HYDROCARBONS OVER AN H-ZSM5 ZEOLITE CATALYST*

4.1 Abstract

The conversion of methyl octanoate on H-ZSM5 zeolite catalysts has been investigated as a model reaction for the production of hydrocarbon fuels and chemicals from biodiesel. The reactivity of methyl octanoate on H-ZSM5 is higher than that observed with a linear alkane of the same chain length, n-octane. The enhanced activity may be due to the strong adsorption of the ester group on the zeolite sites. The deoxygenation of methyl octanoate yielded a variety of hydrocarbons (C_1–C_7), with significant amounts of aromatics. Octanoic acid and heavy products, particularly 8-pentadecanone, were formed as primary products from methyl octanoate via acid-catalyzed hydrolysis and condensation, respectively. Both octanoic acid and the condensation products undergo further reaction, producing aromatics. The comparison conducted with n-octane as a feed indicates that aromatics can be formed through a series of reactions, namely cracking, oligomerization, and cyclization. A small amount of ethylbenzene and o-xylene at low conversion of methyl octanoate indicates that direct dehydrocyclization may also take place, but this path was not evident when the feed was n-octane.

Keywords: Biofuels; Methyl ester conversion; Alkane conversion; Aromatization; H-ZSM5

---

* Applied Catalysis A: General, 361 (2009) 99-105

4.2 Introduction

Fatty acid methyl esters (FAMEs) obtained from the transesterification of triglyceride with methanol have received considerable attention as replacements for fossil fuels [1 - 4]. Advantages of these renewable biodiesels compared to conventional petroleum-derived diesel include their high cetane number, low sulfur content, high flash point, and the cleanness of the exhaust emissions. However, one of the major technical concerns for the biofuels includes the oxidative and thermal instability due to the presence of oxygen [5-8]. The elimination of the oxygen content in biodiesel improves its stability and enhances its utilization potential.

Typically, the deoxygenation of oxygen-containing compounds has been conducted on noble metal catalysts. For instance, Pd/C has been found to be an effective catalyst for the deoxygenation of oxygenates (such as alcohol, carboxylic acid, and ketones) to hydrocarbons [9]. Hydrotreating catalysts, such as CoMo and NiMo supported on Al_2O_3, have also been used for ester deoxygenation under typically high operating pressures [10-12]. To reduce the severity of the operation, several attempts have been made to utilize acid catalysts and transform the oxygen-containing molecules at lower pressures [13, 14].

Among the most common acid zeolite catalysts, H-ZSM5 is well known for its remarkable activity for the conversion of alcohols into hydrocarbons [15], which has been demonstrated in many processes, including MTG, MTO, BTG, and BETE [16, 17]. The hydrocarbons obtained from the reaction are typically in the gasoline boiling range, with substantial amounts of aromatics. Similarly, several reports have demonstrated the successful application of H-ZSM5 for the transformation of other oxygenates (e.g. acetone) to higher paraffins and olefins [18, 19]. The transformation of ketones involves direct decarbonylation to the corresponding olefins in the first step, followed by oligomerization of the olefin. A comparison of the relative reactivities of aldehydes, ketones, and acids on H-ZSM5 has shown that all of them produce olefins and aromatics at high temperatures, but acids are significantly more reactive than aldehydes and ketones [20]. The deoxygenation of these compounds takes place mainly through decarboxylation and dehydration. Recent studies by Corma *et al.* [21] and Huber et al. [22] have shown that H-ZSM5 is an effective

catalyst for the conversion of glycerol and sorbitol. In summary, while deoxygenation on H-ZSM5 has been extensively investigated with alcohols, aldehydes, ketones, and biomass-derived sugars, it has been much less studied with biodiesel esters. Hence, in this work, the conversion of methyl octanoate, as a model biodiesel fuel, has been investigated on H-ZSM5. While methyl octanoate is much shorter than the typical esters present in biodiesel, it contains the important chemical functionality (CH_3-O-COR) that we are interested in investigating. In addition, having a shorter aliphatic chain makes the analysis and handling much easier than working with esters of longer chains. At the same time, we have compared the product distribution from this ester with that resulting from an alkane with the same chain length.

4.3 Experimental

4.3.1 Catalyst Preparation

The H-ZSM5 zeolite catalyst was synthesized following published conventional methods [23] using tetrapropylammoniumbromide (TPABr) as the organic template. The synthesized zeolite was calcined in air at 873 K for 5 h to decompose the organic templates. The resulting Na^+ ions in the synthesized zeolite was replaced with NH_4^+ ions by ion exchange with 1 M NH_4NO_3 solution at 353 K for 10 h, using a liquid/solid ratio of 100 ml per gram of zeolite. Then, the zeolite was separated from the solution by filtering and was thoroughly washing. The exchange procedure was repeated three times to complete the Na^+ ion exchange. Subsequently, the catalyst was dried overnight at 383 K and calcined in flowing dry air at 773 K for 5 h to produce the acidic form of the zeolites (H-ZSM5).

4.3.2 Catalyst Characterization

To confirm the zeolite structure and evaluate the crystallinity of the catalysts, XRD was conducted on all samples using a Rigaku X-Ray Diffractometer with filtered CuK_α line at a scanning rate of 5°/s. Moreover, the zeolite morphology

and crystallite size were investigated in a JEOL 5200-2AE SEM scanning electron microscope. Nitrogen adsorption was carried out at 77 K to obtain the BET area of the synthesized H-ZSM5 zeolite catalysts using a Thermo Finnigan Modeled Sorptomatic 1100 series. Elemental analyses were carried out in a PerkinElmer Optima 4300 DV inductively coupled plasma optical emission spectrometer (ICP-OES).

The zeolite acidity was quantified by the amine TPD (temperature programmed desorption) technique developed by Gorte *et al.* [24]. The sample (30 mg) was initially pretreated in a flow of He for 1 h at 773 K. Then, the sample was cooled in He to room temperature and 10 μl pulses of propylamine were injected over the sample each time until the sample was saturated. The saturation of propylamine adsorption was confirmed by mass spectrometry. After removal of the excess propylamine by flowing He for 3 h, the sample was linearly heated to 973 K at a ramping rate of 10 K/min. Masses 30, 41, and 17 were monitored to determine the evolution of propylamine, propylene, and ammonia, respectively. The amount of desorbed propylene was calibrated with a 5 ml pulse of 2% propylene in He.

The density and strength of the acidic sites of the catalyst were also characterized by FTIR using pyridine as a probe molecule. Infrared spectroscopic measurements of the adsorbed pyridine (Py-IR) were recorded in a Bruker Equinox 55 spectrometer. The sample (90 mg) was pressed into a 2.5 cm diameter self-supported wafer, placed in a gas-tight cell with CaF_2 windows. Prior to pyridine adsorption, the sample was pretreated in a He flow at 773 K for 2 h. After the pretreatment, the sample was cooled to 423 K, and a blank spectrum was taken. Subsequently, pyridine vapor was introduced into the cell and kept for 2 h in order to saturate the acid sites. The excess pyridine was then purged from the cell by flowing He for 12 h. Four spectra were obtained for each sample at 423 K, both on the saturated sample, and after outgassing at increasing temperatures from 573 to 773 K. The absorption band appearing at 1,545 cm^{-1} was assigned to the pyridinium ion formed on the Brønsted acid sites, while the band at 1,455 cm^{-1} was assigned to pyridine coordinated to Lewis acid sites. The density of both Brønsted and Lewis acid sites was then quantified by integrating the corresponding absorption bands and using the molar extinction coefficients proposed by Emeis [25].

4.3.3 Catalytic Activity Measurements

The catalytic activity tests for the reaction of methyl octanoate were performed in a ¼ inch quartz tube at 673 K and 773 K, at atmospheric pressure. To investigate the selectivities of the products as a function of methyl octanoate (MEO) conversion, the space time (W/F) was varied from 0.2 to 6.4 $g_{cat}.h/mol_{MEO}$ in a single-pass continuous flow reactor packed with catalyst powder. Prior to the reaction, the catalysts were treated *in situ* for 1 h in flowing H_2 at the reaction temperature. Methyl octanoate was injected using a syringe pump through a heated vaporization port. The molar ratio of H_2 to feed was kept at 6:1 in all experiments. The products were analyzed by online gas chromatography (Shimadzu GC-17A) using a temperature program to optimize product separation, and a GC/MS (Shimadzu Q5000) for product identification.

4.4 Results and Discussion

4.4.1 Catalyst Characterization

The physical properties of the synthesized H-ZSM5 catalyst obtained by XRD, SEM, and nitrogen adsorption are summarized in Table 4.1. The XRD patterns were fully consistent with those reported in the literature for pure H-ZSM5 [23, 26]. The approximate crystallite size determined by SEM was 3 μm. Chemical analysis indicated that the Si/Al ratio was 36, which corresponds to a maximum theoretical Brønsted acidity density of 450 $\mu mol/g_{cat}$. In good agreement, the TPD of propylamine resulted in a density of accessible sites of 382 $\mu mol/g_{cat}$. The distribution of Brønsted and Lewis sites as a function of temperature as measured by FTIR of adsorbed pyridine is presented in Table 4.2.

Table 4.1 Physical properties of the H-ZSM5 catalyst

	H-ZSM5
Si/Al from chemical analysis	36
BET Surface area (m^2/g)	377
Particle size (μm) from SEM	~ 3
Acidity density ($\mu mol/g_{cat}$) from TPD of isopropylamine	382

Table 4.2 Acidity characterization of H-ZSM5 using the FTIR of adsorbed pyridine

Acidity ($\mu mol\ Py/g_{cat}$)	**Desorption Temperature**			
	423 K	**573 K**	**673 K**	**773 K**
Brønsted (band at 1,545 cm^{-1})	176	90	48	35
Lewis (band at 1,445 cm^{-1})	37	11	8	5

4.4.2 Conversion of Methyl Octanoate

The conversions of methyl octanoate as a function of time on stream at 673 K and 773 K are shown in Figure 4.1. It can be seen that at 673 K, a rapid deactivation is evident. At 773 K, the amount of catalyst used is in excess and 100% conversion was observed for a few hours, until the deactivation was apparent. The product distribution varies with the level of conversion and the reaction temperature. First, Table 4.3 compares the products obtained at the same W/F and same time on stream. It shows that at 773 K, working with excess catalyst, C_2 and C_3 hydrocarbons are the dominant products. In addition, a significant amount of aromatics (i.e. toluene, C_8 aromatics and C_9+ aromatics) were observed. By contrast, at 673 K at the same W/F and same time on stream, the conversion is much lower and octanoic acid and condensation products (namely 8-pentadecanone, pentadecene, and condensation ester) were the major products. Much lower yields of total aromatics were obtained at this temperature.

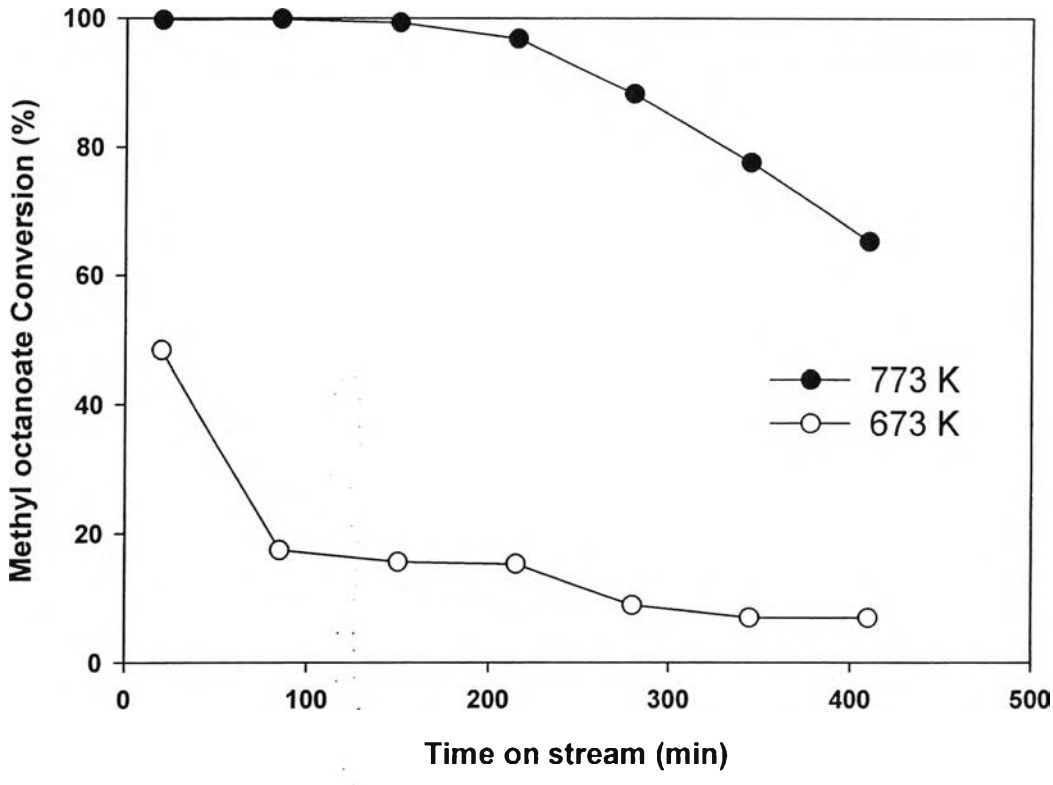

Figure 4.1 Conversion of methyl octanoate over H-ZSM5 as a function of time on stream, at a space time W/F = 6.4 $g_{cat}.h/mol_{MEO}$

Second, an analogous comparison of product distribution at the two temperatures was made at similar conversion by varying the W/F. This comparison allows us to decide which changes in product distribution are due to temperature and which ones are due to the level of conversion. For example, by comparing the data at the same temperature (773 K) and varying conversion, it is clear that the increase in aromatic products is due to an increase in conversion. Little change in selectivity to aromatics is observed when the comparison is done at a similar conversion while varying the temperature. At the same time, the increase in conversion level results in a significant decrease in concentration of octanoic acid and condensation esters in the product, which indicates that these intermediate products are further converted.

Table 4.3 Product distribution from the reaction of methyl octanoate over H-ZSM5 at 673 K and 773 K

Reaction Temperature (K)	**773**	**773**	**673**
W/F (g_{cat}.h/mol_{MEO})	**6.4**	**0.8**	**6.4**
Conversion	99.7	56.5	48.6
Product Selectivity (wt%)			
Methane	6.7	0.5	0.6
C_2	34.3	13.7	3.3
C_3	15.3	1.4	2.2
C_4	5.3	0.2	0.2
C_5	5.8	2.7	0.6
C_6	3.7	1.8	1.0
C_7	2.2	6.5	7.3
Benzene	1.6	0.6	0.6
Toluene	6.2	0.4	0.4
C_8 aromatics			
Ethylbenzene	1.0	0.2	0.1
m-Xylene	8.1	1.0	1.2
p-Xylene	1.8	0.1	0.1
o-Xylene	0.2	0.3	0.1
C_9+ aromatics	2.9	1.6	1.6
Octanal	1.1	0.1	1.0
Octanoic acid	0.4	22.7	50.4
Coupling Products			
Pentadecene	2.6	2.9	16.0
8-pentadecanone	0.6	0.3	0.5
Coupling ester	0.2	43.2	12.8

Reaction Conditions: P = 1 atm, H_2:Feed = 6:1 molar ratio,time on stream = 20 min

The initial total conversion (TOS = 20 min) and product distribution from the reaction of methyl octanoate at 773 K as a function of W/F are shown in Figure 4.2. From the initial slope of the curve at W/F approaching zero, it appears that aromatics are secondary products in this reaction. By contrast, the evolution of 8-pentadecanone and octanoic acid with W/F indicates that these are primary products. The slope at low W/F is positive and their concentrations decrease with W/F after a maximum, indicating that these compounds tend to react further into lighter compounds and aromatics. The distribution of minor products is shown Figure 4.2(c). It is observed that the other condensation products (pentadecene and condensation ester) slowly increase with W/F and they appear to be secondary products.

As previously noted [12], water is a by-product from the deoxygenation of the methylester and can affect the product distribution. To investigate the effect of water, controlled amounts were incorporated in the feed. Figure 4.3 shows the conversion of methyl octanoate as a function of time on stream when different amounts of water were co-fed. It was found that the conversion of methyl octanoate over the H-ZSM5 significantly increased with increasing addition of water. However, by inspecting the slopes in Figure 4.3, one can see that the presence of water does not affect the rate of deactivation. Therefore, it may be inferred that water enhances the catalytic activity of H-ZSM5. To compare the product distribution with and without water addition at comparable conversion levels, we have selected data at various times on stream to match similar conversions (~70%). Table 4.4 shows that while the yield of total aromatics decreases with increasing water content, the yield of octanoic acid increases. It is possible that an increase in the rate of hydrolysis results in higher acid and alcohol concentrations. At the same time, the presence of water in the feed may result in adsorption on acid sites, thus reducing the cracking activity. This reduced cracking activity causes the observed decrease in light products and the enhancement in octanoic acid, which in the presence of water, does not get converted as easily as with the dry feed.

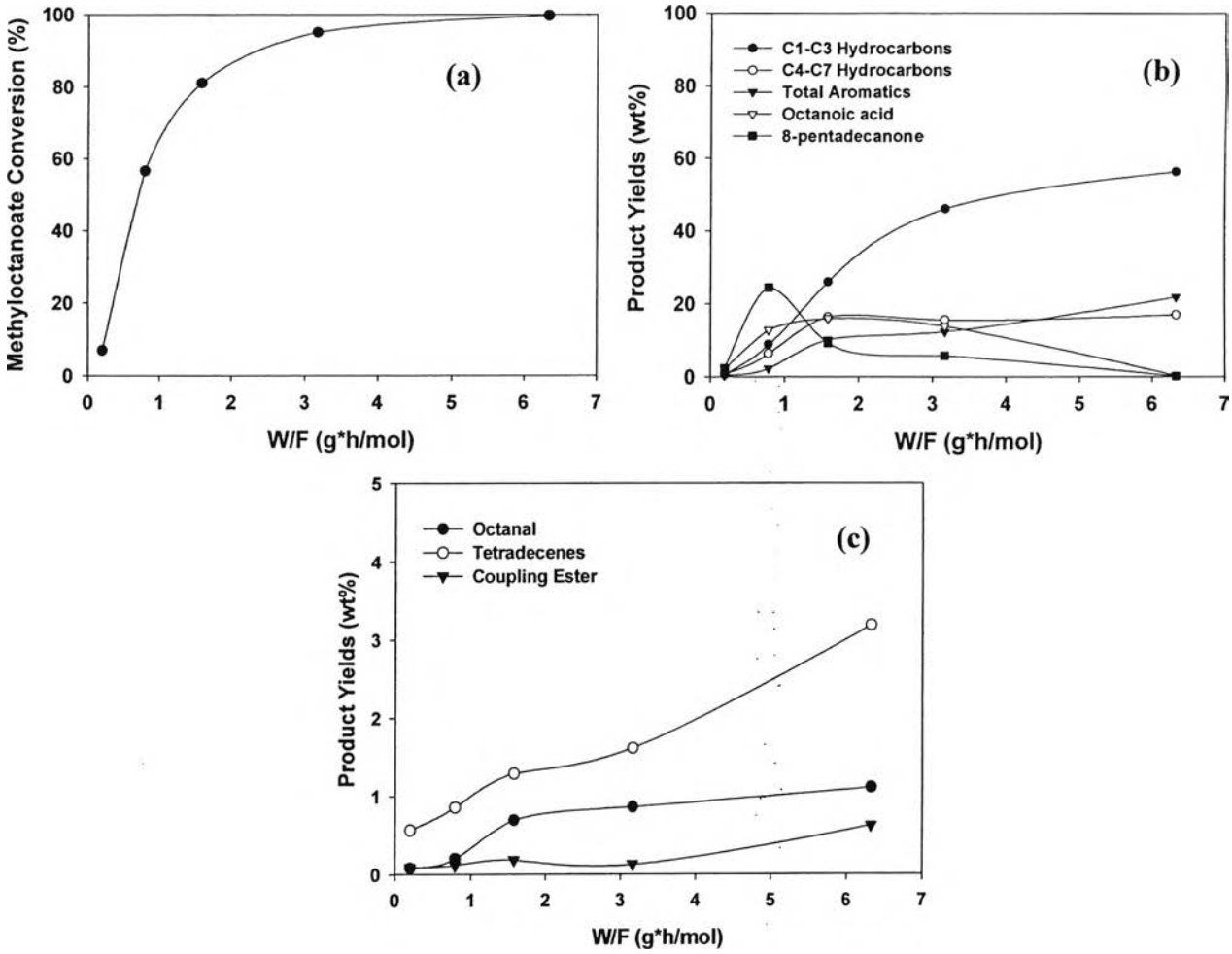

Figure 4.2 Catalytic activity as a function of W/F at 773 K (a) Total methyl octanoate conversion after 20 min on stream; (b) yield of major products; (c) yield of minor products.

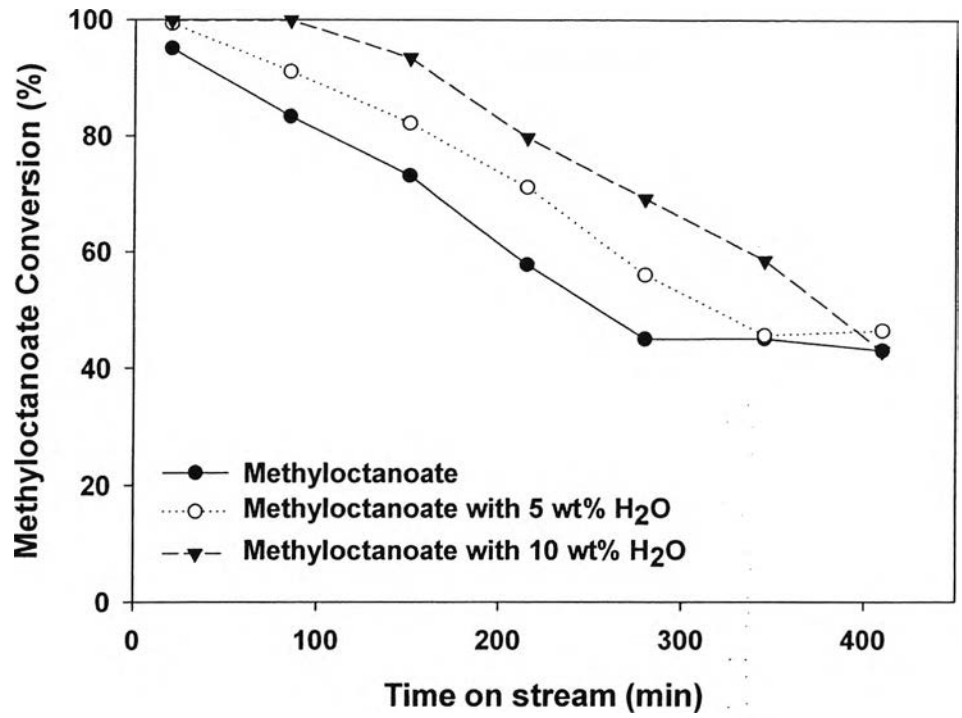

Figure 4.3 Effect of water addition to the feed on the total conversion of methyl octanoate at 773 K.

Table 4.4 Effect of water addition on the product distribution from the reaction of methyl octanoate over H-ZSM5 at 773 K at comparable conversion levels

Water Contents	No Water	5 wt% H_2O	10 wt% H_2O
Conversion	73.1	71.1	69.1
Product Yield (wt%)			
Light hydrocarbons (C_1-C_3)	36.9	25.4	14.2
Heavy hydrocarbons (C_4-C_7)	12.3	11.6	9.2
Aromatics	5.2	3.9	2.6
Octanoic acid	10.6	20.9	28.6
Coupling products	7.9	9.0	14.5

Reaction Conditions: 1 atm, W/F = 3.2 g_{cat}.h/mol_{MEO}, H_2:Feed = 6:1 molar ratio. Time on stream was adjusted to obtain similar conversion levels.

4.4.3 Conversion of n-Octane

To compare the relative activity of methylester and its product distribution with a linear alkane of the same chain length, reaction studies under identical conditions as those with methyl octanoate were conducted with n-octane. The aromatization of alkanes on H-ZSM5 has been widely investigated, and it is well established that it involves a series of steps that include the conversion of alkanes into alkenes, oligomerization of the alkenes, the formation of a common pool of alkene intermediates, and alkene aromatization [27-31].

Comparing the data in Figure 4.4 with those in Figure 4.1, it is seen that the activity for n-octane conversion over the H-ZSM5 in the 673–773K range was substantially lower than that for methyl octanoate conversion at any given temperature. At the same time, it is apparent that the rate of catalyst deactivation is appreciably lower when the alkane is the feed.

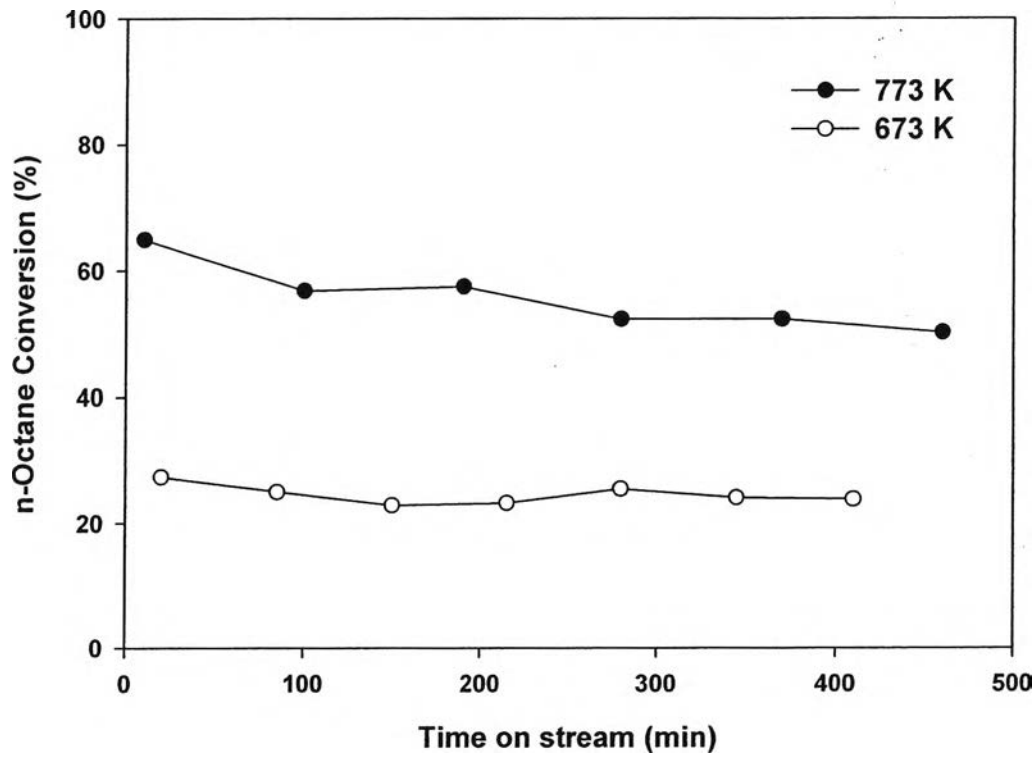

Figure 4.4 Conversion of n-octane over H-ZSM5 as a function of time on stream, at W/F = 6.4 $g_{cat}.h/mol_{n\text{-}C8}$ and two different temperatures, 673 and 773 K.

As summarized in Table 4.5, the product distribution obtained from n-octane at moderate conversions shows C_3 and C_4 hydrocarbons as the dominant products, in agreement with results reported by Abbot and Guerzoni [32]. Aromatic products (namely benzene, toluene, and C_8 aromatics) were also observed, but with much lower selectivity when compared to those produced from the reaction of methyl octanoate at comparable W/F. Interestingly, only m-xylene and p-xylene, with no ethylbenzene and o-xylene, were formed at this condition. In addition, C_9+ aromatics were not observed. As also shown in Table 4.5, the selectivity toward total aromatics is relatively lower at 673 K, while the selectivities to C_5–C_7 hydrocarbons increased. Furthermore, since the methyl octanoate can be converted to heptene/ane, we conducted a comparable study with n-heptane feed, under the same conditions as those with the n-octane feed. As shown in Table 4.5, in this case the C_3 and C_4 hydrocarbons were formed as the major products, which is similar to what was observed in the reaction with n-octane. Benzene and toluene were the aromatic products produced from the reaction of n-heptane. While, it is possible that some contribution of direct aromatization of n-heptane occurs, compared to the reaction of the methyl octanoate, the selectivity to total aromatics was still significantly lower.

Figure 4.5 illustrates the evolution of products as a function of W/F. It is clear that, at low W/F, β-scission is the dominant reaction that produces C_2–C_4 hydrocarbons, with high concentration of olefins. Clearly, the formation of aromatics from n-octane is not a primary reaction, but only occurs after the small hydrocarbon fragments oligomerize and cyclize.

Table 4.5 Product distribution from the reactions of n-heptane and n-octane over H-ZSM5

Feed	**n-Heptane**	**n-Octane**	
Reaction Temperature (K)	**773**	**773**	**673**
Conversion	54.8	64.9	27.0
Product Selectivity (wt%)			
C_1	1.8	0.6	4.3
C_2	13.1	14.2	24.3
C_3	37.6	40.6	32.8
C_4	28.0	28.8	17.0
C_5	9.8	8.7	14.0
C_6	1.3	2.0	4.6
C_7	0.0	0.0	1.2
Benzene	2.5	0.5	0.4
Toluene	5.9	2.4	0.6
C_8 aromatics			
Ethylbenzene	0.0	0.0	0.0
m-Xylene	0.0	1.4	0.6
p-Xylene	0.0	0.8	0.2
o-Xylene	0.0	0.0	0.0

Reaction Conditions: 1 atm, W/F = 6.4 g_{cat}.h/mol, H_2:Feed = 6:1 molar ratio, 20 min after the reaction

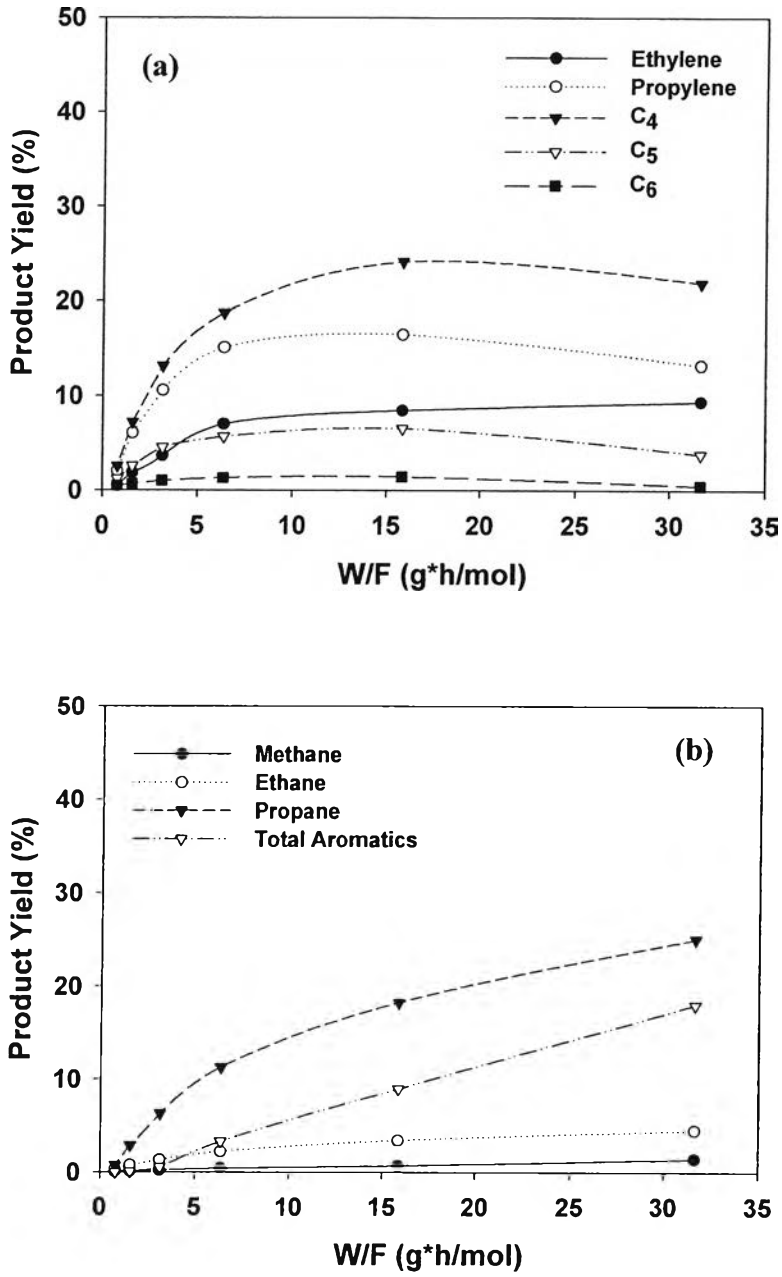

Figure 4.5 Yield of primary products (a) and secondary products (b) obtained from the reaction of n-octane as a function of W/F at 773 K.

4.4.4 The Reactivity Comparison of the Two Different Feeds

We found that to reach a given yield to aromatics, much higher space times were needed with n-octane than with methyl-octanoate. Figure 4.6 shows a remarkable difference between the yield to total aromatics obtained from methyl octanoate and n-octane as a function of W/F. That is, to obtain the same yield of aromatics from n-octane, the W/F needed is between 5 and 10 times higher than that needed when methyl octanoate is the feed.

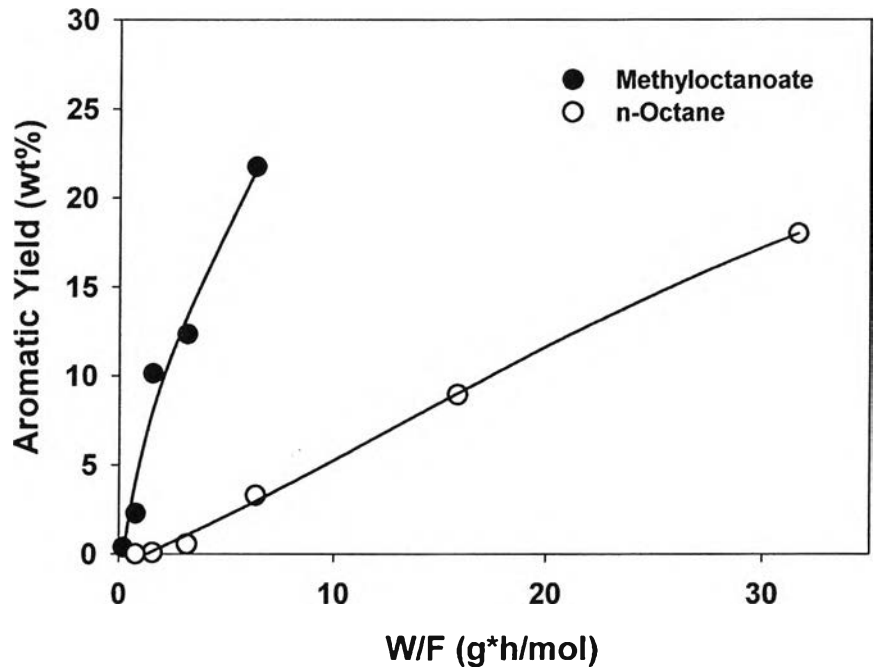

Figure 4.6 Comparison of aromatic yields as a function of W/F obtained from the reaction of methyl octanoate and n-octane over H-ZSM5 catalyst.

To better compare the different reaction paths followed from the two different feeds, the reactions of both methyl octanoate and n-octane were conducted on H-ZSM5 at low conversions (~7%) shown in Table 4.6. From n-octane, the main hydrocarbons obtained at this low conversion are C_3 and C_4, two cracking products which indicate that this alkane is preferentially activated in the middle of the molecule by β-scission [28, 29]. By contrast, the main hydrocarbon product from

methyl octanoate is C_7, which arises from deoxygenation reactions (decarbonylation of the ester or decarboxylation of the acid). The second most abundant hydrocarbon is C_3, which is probably a secondary product from C_7. While no other products are obtained from n-octane, the methyl ester produces significant amounts of octanoic acid and condensation products. Only small amounts of toluene and ethylbenzene/o-xylene, which would be the products of the direct dehydrocyclization of C_7 and C_8, respectively [33, 34], were observed.

Table 4.6 Product distribution from the reactions of methyl octanoate and n-octane at 7% conversion

Feed	**Methyl Octanoate**	**n-Octane**
Product Selectivity (wt%)		
C_1	1.4	0.7
C_2	1.7	10.2
C_3	3.6	35.1
C_4	0.5	32.7
C_5	0.5	15.3
C_6	1.0	5.9
C_7	9.3	0.0
Benzene	0.1	0.0
Toluene	0.1	0.0
C_8 aromatics		
Ethylbenzene	0.1	0.0
m-Xylene	0.2	0.0
p-Xylene	0.1	0.0
o-Xylene	0.1	0.0
C_9+ aromatics	2.3	0.0
Octanal	3.0	0.0
Octanoic acid	31.2	0.0
Coupling Products	44.4	0.0

Reaction Conditions: 773 K, 1 atm, H_2:Feed = 6:1 molar ratio, 20 min after the reaction

Since aromatics are secondary products, a practical way to compare the tendency of a given feedstock to yield the desirable product is to plot the yield of the target product (i.e., aromatics) as a function of the yield to all the other products [35]. Figure 4.7 illustrates the correlation between the yield of non-aromatic hydrocarbons and that of aromatics for the conversion of methyl-octanoate and n-octane on H-ZSM5. It is clear that, at low conversions for a given yield of aromatics, the yield of non-aromatics is much higher for the n-octane feed than for the methyl ester, which illustrates the higher tendency of the non-aromatics produced from methyl octanoate to go to aromatics than those produced from n-octane.

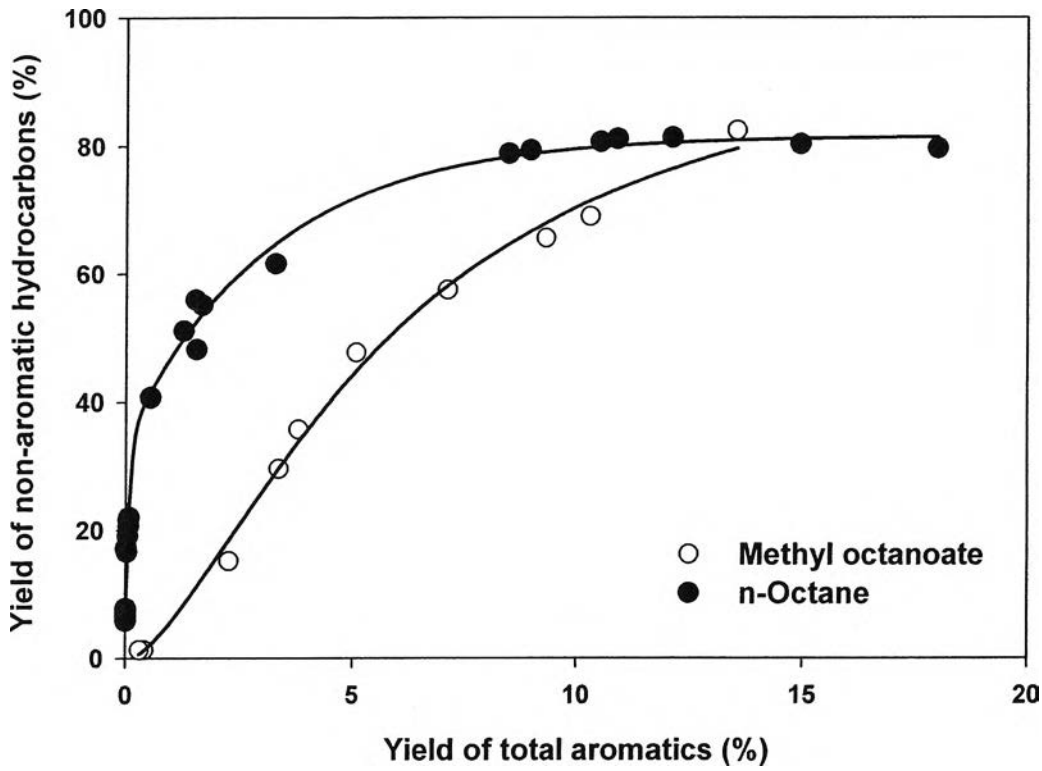

Figure 4.7 Correlation yield of non-aromatic hydrocarbons as a function of yield of aromatics obtained from the reactions of methyl octanoate and n-octane over the H-ZSM5 catalyst.

The higher activity observed with methyl octanoate may be related to the stronger adsorption and higher reactivity of the oxygenated intermediates on the acid sites of H-ZSM5, as one can expect [36]. It is apparent that oxygenates can produce

surface intermediates that can cyclize more effectively than the smaller fragments from the n-octane cracking, which need to undergo oligomerization before formation of the aromatic rings. As observed in the low-conversion measurements, methyl octanoate yields condensation compounds as the dominant primary products. High molecular weight products may be produced by the condensation of adsorbed methyl octanoate, forming dioctanoic acid anhydride and dimethyl ether (DME) as a by-product, in line with recent observations [37]. The 8-pentadecanone is likely to remain on the surface long enough for further reactions because of its low mobility. It could undergo the dehydration reaction, producing a long chain inner olefin, namely pentadecenes, as well as cracking. In fact, the yield of 8-pentadecanone readily decreases with increasing W/F, in parallel with the increase in the yield of pentadecene. In addition, the dehydration of DME yields light olefins and water on acid catalysts [38, 39].

The formation of octanoic acid at low methyl octanoate conversions suggests that hydrolysis of the ester is an initial reaction path on H-ZSM5. Hydrolysis produces the carboxylic acid and alcohol (that is, the reverse reaction of the well-known acid-catalyzed esterification [36,40,41]). The significant increase in octanoic acid yield observed when water was added supports the participation of this reaction. However, there is no water present in the feed; water may arise from the decomposition of DME and the dehydration of 8-pentadecanone during the reaction.

The situation with the n-alkane feed is entirely different. Only cracking of n-octane takes place as the primary reaction over H-ZSM5 [42]. As shown in Figure 4.5, as W/F increases, the cracking products appear to undergo oligomerization, followed by cyclization to aromatics. That is, with alkane as a feed, it is necessary that it undergocracking to generate olefins leading to carbenium ions that have a residence time on the surface long enough to result in oligomerization and cyclization. By contrast, with the methyl ester, the oxygenated reaction intermediates exhibit stronger interactions with the acid catalyst, lower mobility, and longer residence time on the surface. First, the decarboxylation of acids or the decarbonylation of esters directly leads to olefins as the dominant products [43, 44]. Second, the low mobility of the condensation products yield help the molecules stay on the surface long enough for secondary reactions. Accordingly, such molecules can

be converted to aromatics by direct dehydrocyclization and the sequential reactions for aromatization. Consistent with these differences, higher yields to total aromatics were obtained from the methyl ester.

From the analysis of the product distributions of methyl octanoate and n-octane over H-ZSM5 as a function of W/F, several possible reaction pathways of the reactions can be proposed, as summarized in Figure 4.8. The conversion of the ester follows three parallel paths that start with self-condensation and hydrolysis, respectively. The condensation products can undergo subsequent reactions to form both non-aromatic and aromatic secondary products. For the second path, the water required for the hydrolysis of ester can be supplied from the dehydration of condensation products and the subsequent decomposition of DME. The octanoic acid formed by this route can be decarboxylated/decarbonylated forming olefins, which are incorporated to the common olefin pool, eventually becoming aromatics. The third path involves in the direct dehydrocylization of the methylester to aromatics.

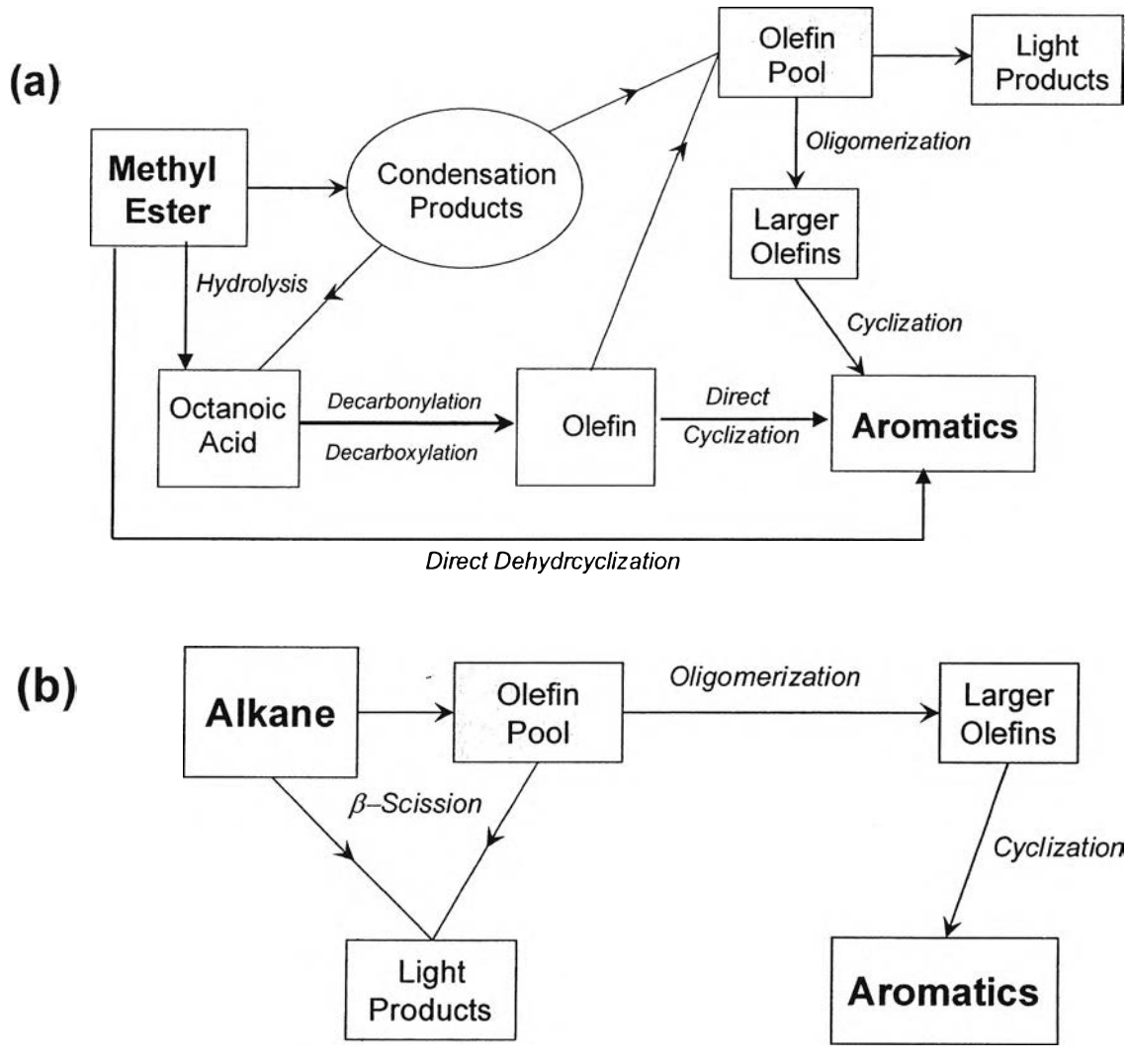

Figure 4.8 Proposed reaction scheme for the conversion of (a) methyl octanoate and (b) n-octane over the H-ZSM5 catalyst.

4.5 Conclusions

Aromatization on H-ZSM5 occurs much more effectively from methyl octanoate than from n-octane. The deoxygenation of the methyl octanoate initially proceeds through condensation and hydrolysis, forming a high molecular weight ketone (8-pentadecanone) and octanoic acid. Hydrocarbons are produced from the cracking reaction of the 8-pentadecanone and octanoic acid. By contrast, the formation of aromatics from n-octane takes place via cracking that leads to the formation of an olefin pool, followed by oligomerization and cyclization.

4.6 Acknowledgements

This contribution has been financially supported by the Oklahoma Secretary of Energy, the Oklahoma Bioenergy Center, the Thailand Research Fund (TRF) under the Royal Golden Jubilee Ph.D. programs, the Center for Petroleum, Petrochemicals, and Advanced Materials (PPAM), and the Petrochemical and Environmental Catalysis Research Unit of the Ratchadapiseksompote Endowment.

4.7 References

[1] I. N. Martynov, A. Sayari, Appl. Catal. A 339 (2008) 45

[2] D. G. Aranda, R. T. P. Santos, N. C. O. Tanpanes, A. L. D. Ramos, O. A. C. Antunes, Catal. Lett. 122 (2008) 20

[3] D. E. Lopez, K. Suwannakarn, D. A. Bruce, J. G. Goodwin Jr., J. Catal. 247 (2007) 43

[4] M. D. Serio, R. Tesser, L. Pengmei, E. Santacesaria, Energy & Fuels 22 (2008) 2007

[5] G. Knothe, Energy Fuels 22 (2008) 1358

[6] G. Knothe, Fuel Process. Technol., 86 (2005) 1059

[7] G. Knothe, A. C. Matheaus, T.W. Ryan III, Fuel 82 (2003) 971

[8] G. Knothe, Fuel Process. Technol., 88 (2007) 669

[9] P. Maki-Arvela, I. Kubickova, M. Snare, K. Eranen, D.Y. Murzin, Energy Fuels 21(2007) 30

[10] E. Furimsky, Appl. Catal. A. 199 (2000) 147

[11] O. I. Senol, T. R. Viljava, A. O. I. Krause, Catal. Today 100 (2005) 331

[12] O. I. Senol, T. R. Viljava, A. O. I. Krause, Catal. Today 106 (2005) 186

[13] J. D. Adjave, N. N. Bakhshi, Fuel Proc. Techno. 45 (1995) 161

[14] J. D. Adjave, N. N. Bakhshi, Energy Fuel 9 (1995) 1605

[15] P. Dejaifve, J. C. Vedrine, V. Bolis, E. G. Derouane, J. Catal. 63 (1980) 331

[16] W. Wang, Y. Jiang, M. Hunger, Catal. Today 116 (2006) 102

[17] R. Le Van Mao, P. Levesque, G. McLaughlin, L. H. Do, Appl. Catal. 34 (1987) 163

[18] G. J. Hutchings, P. Johnston, D. F. Lee, C. D. Williams, Catal. Lett. 21 (1993) 49

[19] A. G. Gayubo, A. T. Aguayo, Atutxa, R. Prieto, J. Bilbao, Energy Fuel 18 (2004) 1640

[20] A. G. Gayubo, A. T. Aguayo, Atutxa, R. Agudo, M. Olazar, J. Bilbao, Ind. Eng. Chem. Res. 43 (2004) 2619

[21] A. Corma, G. W. Huber, L. Sauvanaud, P. O'Connor , J. Catal. 247 (2007) 307

[22] A. Corma, G. W. Huber, L. Sauvanaud, P. O'Connor , J. Catal. 257 (2008) 163–171

[23] R. J. Argauer, G. R. Landolt, US Patent 3 702 886 (1972)

[24] D. J. Parrillo, A. T. Adamo, G. T. Kokotailo, R. J. Gorte, Appl. Catal., 67 (1990) 107

[25] C. A. Emeis, J. Catal. 141 (1993) 347

[26] M. M. J. Treacy, J. B. Higgins, Collections of Simulated XRD Powder Patterns for Zeolites (5th Ed.), 2007, Elsevier, pp. 278

[27] L. H. Nguyen, T. Vazhnova, S. T. Kolaczkowski, D. B. Lukyanov, Chem. Eng. Sci. 61 (2006) 5881

[28] Biscardi, J.A., Iglesia, E., J. Phys. Chem. B 102 (1998) 9284

[29] Biscardi, J.A., Iglesia, E., J. Catal. 182 (1999) 117

[30] Guisnet, M., Gnep, N. S., Appl. Catal. A 146 (1996) 33

[31] Guisnet, M., Gnep, N. S., Alario, F., Appl. Catal. 89 (1992) 1

[32] J. Abbot and F. N. Guerzoni, Appl. Catal. A., 85 (1992) 173

[33] B. H. Davis, J. Catal. 42 (1976) 376

[34] F. G. Gault, Adv. Catal. 30 (1981) 1

[35] G. Jacobs, C. L. Padro, and D. E. Resasco, J. Catal. 179 (1998) 43

[36] S. Patai in The Chemistry of Carboxylic Acids and Esters, Interscience, New York, (1969).

[37] M. Glinski, W. Szymanski, D. Lomot, Appl. Catal. A 281 (2005) 107

[38] M. Stocker, Micropor. Mesopor. Mater., 29 (1999) 3

[39] C. D. Chang, A. J. Silvestri, J. Catal 47 (1977) 249

[40] S.H. Hilal, S. W. Karickhoff, L. A. Carreira, B. P. Shrestha, QSAR Comb. Sci. 22 (2003) 917

[41] M. A. Ogliaruso, J. F. Wolfe, Synthesis of Carboxylic Acid, Esters And Their Derivatives, John Wiley & Sons, New York, 1991

[42] S. Kotrel, H. Knozinger, B. C. Gates, Micropor. Mesopor. Mater. 35-36 (2000) 11

[43] T. Sooknoi, T. Danuthai, L. L. Lobban, R. G. Mallinson, D. E. Resasco, J. Catal 258 (2008) 199

[44] M. Snare, I. Kubickova, P. Maki-Arvela, D. Chichova, K. Eranene, D. Y. Murzin, Fuel 87 (2008) 933